

Cross-sectioning spatio-temporal Co-In electrodeposits: disclosing a magnetically-patterned nanolaminated structure

Irati Golvano-Escobal¹, Juan de Dios Sirvent¹, Marta Ferran-Marqués¹, Santiago Suriñach¹, Maria Dolors Baró¹, Salvador Pané², Jordi Sort^{1,3,}, Eva Pellicer^{1,*}*

¹Departament de Física, Universitat Autònoma de Barcelona, E-08193 Bellaterra, Spain

²Institute of Robotics and Intelligent Systems (IRIS), ETH Zürich, CH-8092 Zürich, Switzerland

³Institució Catalana de Recerca i Estudis Avançats (ICREA), Pg. Lluís Companys 23, E-08010 Barcelona, Spain

* Jordi.Sort@uab.cat; Eva.Pellicer@uab.cat

Abstract

Micrometer-thick cobalt-indium (Co-In) films consisting of self-assembled layers parallel to the cathode plane, and with a periodicity of 175 ± 25 nm, have been fabricated by electrodeposition at a constant current density. These films, which exhibit spatio-temporal patterns on the surface, grow following a layer-by-layer mode. Films cross-sections were characterized by electron microscopies and electron energy loss spectroscopy. Results indicate the spontaneous formation of nanolayers that span the whole deposit thickness. A columnar structure was revealed inside each individual nanolayer which, in turn, was composed of well-distinguished In- and Co-rich regions. Due to the dissimilar magnetic character of these regions, a periodic magnetic nanopatterning was observed in the cross-sectioned films, as shown by magnetic force microscopy studies.

Keywords: Co-In nanolaminates, electrodeposition, electron energy loss spectroscopy, magnetic force microscopy.

1. Introduction

Nanolaminates, defined as stacks of alternating ultra-thin layers of different materials, hold great promise for several applications requiring outstanding mechanical properties [1,2], optical [3] and magnetic features [4]. Moreover, since nanolaminates are frequently made of metal oxides, they find uses in biomedical devices requiring biocompatible materials [5]. Several approaches including sputtering [6,7], atomic layer deposition (ALD) [8,9], pulsed-laser deposition (PLD) [10], physical vapor deposition [11], ball-milling [12] and electrodeposition [4,13-15] have been adopted to produce composite films made of alternated layers. Sputtering, ALD and PLD processes are relatively common deposition techniques but they have a few disadvantages. Namely, residual stress during films' growth yield coatings with poor mechanical properties. This often leads to cracking, buckling, or delamination of the nanolaminates [16,17]. Besides, the deposition rates are rather slow. Electrodeposition has been widely utilized to produce micrometer-thick structures composed of alternated layers (metals, alloys and even polymers) in different configurations (films, rods and wires). Because it works at room pressure and temperature, electrodeposition possesses many attractive features like low cost and industrial scalability [18]. Layered coatings are typically fabricated from a single electrolyte by conveniently switching the deposition potential or current density [19] or by using different electrolytes [20]. The former approach is preferred when smaller layer thicknesses and a high number of repetitions are desired.

The in-situ formation of spatio-temporal patterns during the electrodeposition of some binary systems such as Ag-Bi, Ag-Cd, Ag-In, Ag-Sb or Co-In was previously demonstrated [21-27]. The spatio-temporal patterns typically consist of a mixture of waves, targets and spirals whose relative proportion was shown to depend on a number of factors, such as the nature of the system and the applied current density. Interestingly, it was recently found that the Co-In system not only exhibits the spatio-temporal self-pattern on the surface, but also a fancy layer-by-layer growth type [28]. Although the spontaneous formation of layered deposits with a repeat length of tens or hundreds of nanometers has been observed in a quite few instances [29-31], this growth mode in immiscible systems exhibiting spatio-temporal patterns has not been studied in detail.

The aim of this work is to characterize the layer-by-layer growth in electrodeposited spatio-temporal Co-In films using electron microscopy techniques. The goal is to explore the cross-section of the electrodeposits in order to determine whether composition is homogeneous across the nanolayers or, instead, it varies within each layer or from one layer to another. This could eventually lead to dissimilar magnetic properties and hence, confer these materials new technological functionalities. In such a case, Co-In nanolaminates would be spontaneously produced from a single electrolyte under nominally constant conditions, which represents a step forward within the field of electrodeposited multilayered materials.

2. Experimental

Deposition of Co-In coatings was conducted in a three-electrode cell connected to a PGSTAT302N Autolab potentiostat/galvanostat (Ecochemie). A double junction Ag|AgCl ($E=+0.210\text{V}/\text{SHE}$) reference electrode (Metrohm AG) was used with 3M KCl

inner solution and 1M NaCl outer solution. A platinum sheet served as a counter electrode. Silicon (111) substrates with e-beam evaporated Ti (100 nm)/Au (125 nm) adhesion/seed layers were used as cathodes for Co-In growth. The working area of the Au/Ti/Si substrates was $5 \times 5 \text{ mm}^2$. Co-In deposits of 10 μm in thickness were obtained at constant current densities from -10 mA cm^{-2} to -20 mA cm^{-2} .

The on-top morphology of the films was characterized with a Zeiss Merlin field emission scanning electron microscope (FE-SEM). The average Co content in the coatings was determined by energy dispersive X-ray spectroscopy (EDX) operated at 20kV. The structure of the films was determined by X-ray diffraction (XRD) using a Philips X'Pert Diffractometer in Bragg–Brentano geometry using Cu $K\alpha$ radiation (note that both wavelengths $\lambda(K_{\alpha 1}) = 1.5406 \text{ \AA}$ and $\lambda(K_{\alpha 2}) = 1.5443 \text{ \AA}$ were used in intensity proportion of $I(K_{\alpha 2}) = I(K_{\alpha 1}) = 0.5$) in the $25\text{--}125^\circ$ 2θ range (0.03° step size and 10 s holding time). Films' cross-section was prepared differently depending on whether transmission electron microscopy (TEM) or FE-SEM was targeted. For TEM purposes, cross-sections were prepared by embedding the film in epoxy resist followed by cutting thin slices with an ultramicrotome (Leica EM UC6, Leica Microsystems Ltd., Milton Keynes, UK) using a 35° diamond knife at room temperature. Analyses were performed on a FEI Tecnai20 high-resolution S/TEM operated at 200 kV, equipped with energy dispersive X-ray detector. For SEM analyses (Zeiss Merlin), the films were embedded in a conductive epoxy resin, grinded to remove the resin, and polished using Struers MD-Largo composite disc onto which 9 μm water based diamond suspension was applied. The room temperature magnetic properties were measured using a vibrating sample magnetometer (VSM) from Oxford Instruments. Hysteresis loops were recorded under a maximum applied field of 700 Oe applied along the parallel and perpendicular-to-plane directions. Atomic and magnetic force microscopy (AFM/MFM) images were

acquired using Dual Scope C-26 system from Danish Micro Engineering. The MFM maps were taken at a tip lift height of 100 nm.

3. Results and discussion

The structural characterization was studied by XRD (Figure S1, Supporting information) and revealed reflections assigned to tetragonal In, tetragonal CoIn_3 , face-centered cubic Co and hexagonal-close packed Co. FE-SEM images of the on-top and cross-section morphologies of the Co-In films are shown in **Figure 1**. While the top view of the films (Figure 1a) show spatio-temporal patterns with micrometer lateral sizes consisting of a mixture of spirals, waves and targets spread all over the surface, the film's cross-section (Figure 1b) displays a layer-by-layer nanoarchitecture. Such a multilayered structure was seen in all coatings deposited at current densities between -10 and -20 mA cm^{-2} , corresponding to average Co contents ranging from 25 to 90 at%. Remarkably, this layered arrangement was also observed in cross-sectioned Ag-Sb electrodeposited coatings exhibiting surface spatio-temporal patterns [32]. According to the authors, current oscillations recorded during stationary potentiostatic deposition corresponded to the formation of coarse travelling waves consisting of phases with different Sb content and their propagation in front of the Haber-Luggin capillary. This led to the formation of layered structures visible in the cross-sections of the deposits. Although most of the investigated systems with self-organization phenomena during electrodeposition show either current or potential oscillations, Co-In system E-t transients are characterized by a spike during the first seconds of deposition, followed in all cases by relaxation of the potential towards a rather stationary value, without any oscillation (Figure S2, Supporting information).

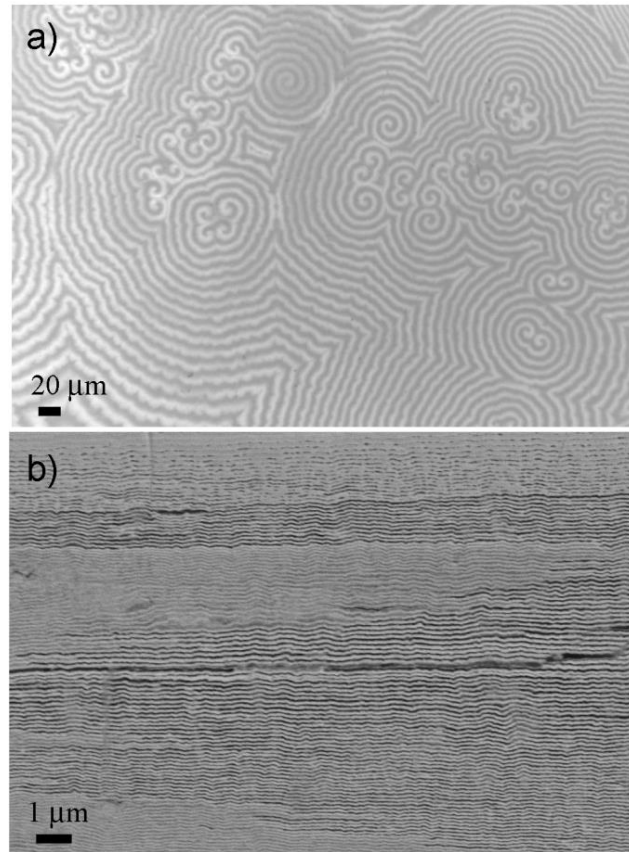


Figure 1. SEM images of a Co-In coating obtained at $j = -12 \text{ mA cm}^{-2}$ (58 at% Co) a) top view and b) cross section.

A closer look to the cross-section of the Co-In films was taken by TEM working on STEM mode (**Figure 2**). The formation of partially stacked individual layers, undulated and rather uniform in thickness was observed, in agreement with previous SEM analyses (Figure 2a and 2b). Interestingly, a kind of columnar structure is observed in each nanolayer (Figure 2c). Such a columnar grain structure is often observed in electrodeposited metals and alloys [33]. The repetition length as measured by TEM was $175 \text{ nm} \pm 25 \text{ nm}$ across the entire deposit thickness, thus furnishing a highly, almost perfect, repeatable 2D pattern expanding several micrometers. Three regions were distinguished within each layer. Namely, a wider, dense, bright region followed by a more irregular, fluffy, grey region, and finally a dark area (Figure 2c). EDX line scan analyses across two adjacent nanolayers were conducted in order to shed light on the

chemical composition profile (Figure 3a). The above-mentioned heterogeneity was evident as the beam was scanning from the center of one nanolayer toward the center of the adjacent nanolayer (Figure 3b). The relatively dense bright area was enriched in In whereas the spongy-like grey area contained a larger amount of Co on average, although the In and Co signals strongly fluctuate. Remarkably, the dark regions correspond to areas mainly free from material. STEM-EDX line scan analyses across these dark regions confirmed the occurrence of holes in the material (Figure S1 and S2, Supporting information). Eventual delamination during sample preparation (cutting by ultramicrotome) for STEM analyses that could explain the existence of these gaps is unlikely. Therefore, such apparently ‘empty’ regions already develop during film deposition. Interestingly, lateral growth is favored over vertical growth in spite of these discontinuities. The occurrence of In- and Co-rich regions was observed in different areas of the cross-sectioned films and therefore was proven neither to be an artifact of the measurement nor an anomaly of the deposit in the region of interest. It was also observed that the nanolayers were joined together mostly through In-rich anchor points (see Figures 2b and 2d).

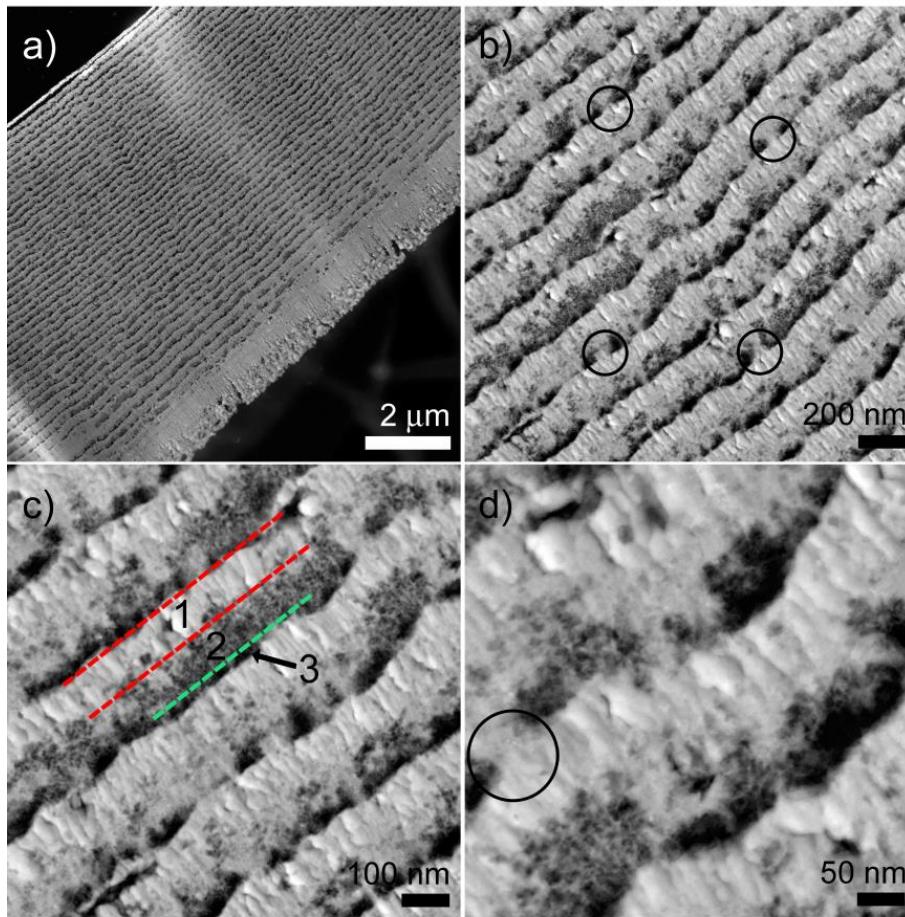


Figure 2. (a-d) STEM micrographs of the cross-section of Co-In coating obtained at $j = -20 \text{ mA cm}^{-2}$ (78 at% Co) at different magnifications. In b) and d) some In-rich anchor points are encircled. In c) the three distinct regions within each layer are indicated.

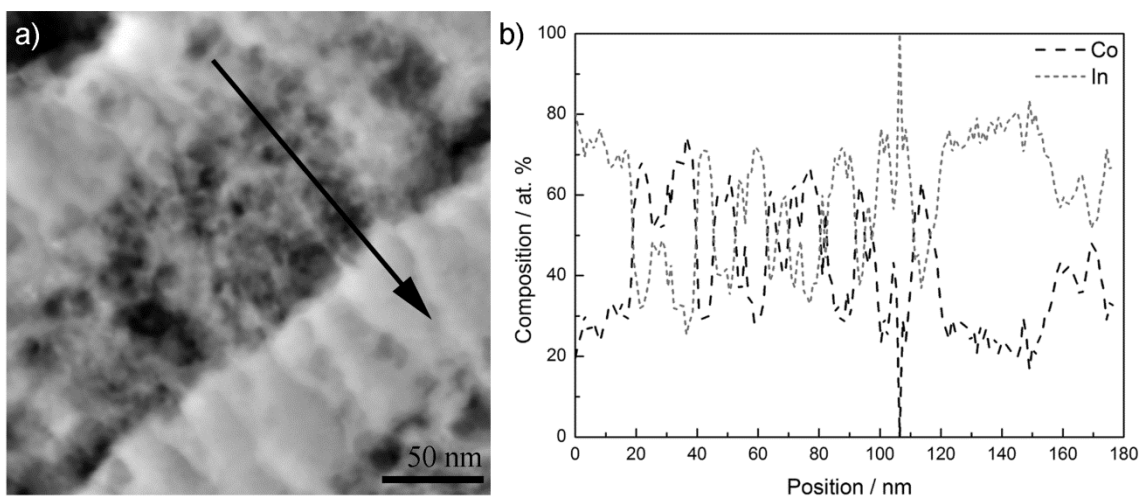


Figure 3. a) STEM micrograph and b) EDX line scan acquired across the black line indicated in a) on the cross-section of a Co-In coating obtained at $j = -20 \text{ mA cm}^{-2}$ (78 at% Co, data obtained from EDX analysis from the FE-SEM).

Previous EDX mappings conducted on the cross-section of a Co-In deposit seemingly indicated that the distribution of Co and In elements was homogeneous [28]. Current EELS analyses do demonstrate that this is not the case and that composition heterogeneities exist at the nanoscale. TEM images of the same region imaged by STEM are displayed in Figure 4a and 4b. Notice that the contrast is opposed to that observed in STEM mode. Bright regions correspond to hollow spaces in the deposit. The HRTEM image (Figure 4c) demonstrates that the material is polycrystalline, in agreement with previous works [28]. It has been claimed that the spatio-temporal structures do move in the vertical direction. This is possibly connected with the effect of natural convection during electrodeposition and results in the formation of layered coatings [32]. Indeed, a zoomed detail of the very first layers deposited on the substrate reveals that when an undulation or a “defect” appears, this is conformally wrapped by the subsequent layers until the growing front becomes flattened (**Figure 5**).

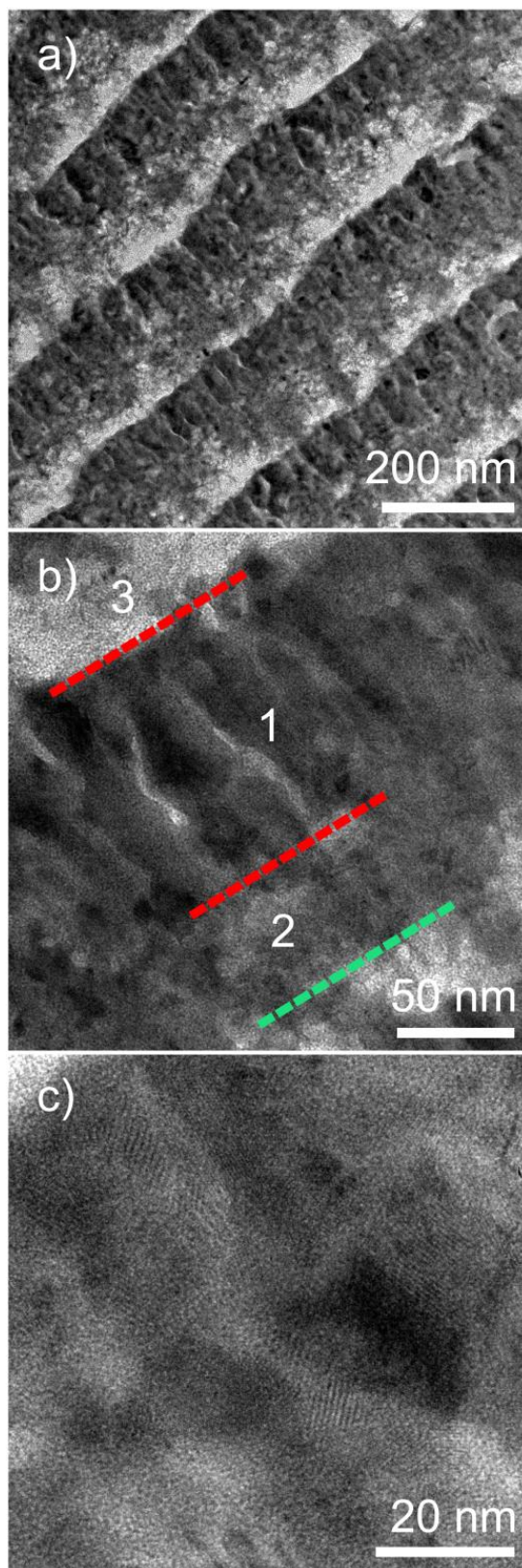


Figure 4. a,b) TEM and c) HRTEM images of the cross-section of a Co-In coating obtained at $j = -20 \text{ mA cm}^{-2}$ (78 at% Co). In b) the three distinct regions within each layer are indicated.

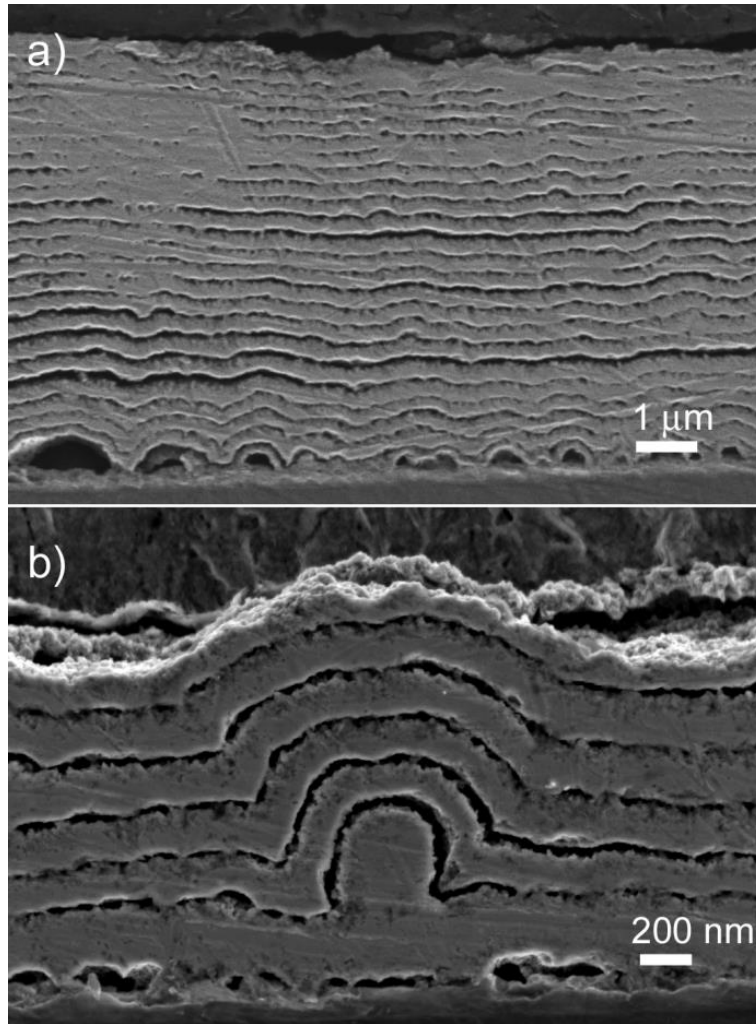


Figure 5. SEM images of a) the cross-section of a Co-In coating obtained at $j = -12 \text{ mA cm}^{-2}$ (58 at% Co) showing undulations at the substrate interface and b) detail of one undulation.

Co-In nanolayered films show a ferromagnetic response at room temperature as has been previously reported [28] and shown here in Figure 6. MFM characterization of the cross-section of the deposits was carried in order to assess any kind of magnetic patterning arising from the layer-by-layer architecture of the Co-In films. **Figure 7a** shows the AFM image obtained upon scanning an area of $1 \times 1 \mu\text{m}^2$, in which the periodical layered structure, already observed by SEM and (S)TEM, was captured. In this topological image, alternating dark and bright fringes are observed, corresponding

to the In-rich and Co-In lamellae. The corresponding MFM image (Figure 7b) was acquired in remanent state after applying a strong magnetic field perpendicular to the film cross-section. In the MFM image, a magnetic nanopatterning is observed, which correlates well with the layered structure seen in Figure 2a. Remarkably, the bright fringes in the AFM image do match the brighter regions in the MFM image, hence evidencing that the MFM contrast is magnetic, rather than topological. Narrower stripes with magnetic contrast likely matching the Co-rich regions (dark bands in STEM) are separated by wider featureless In-rich regions (bright bands in STEM). The local heterogeneity of the cottony-like Co region is though not captured by MFM due to the small size of the compositionally varying regions.

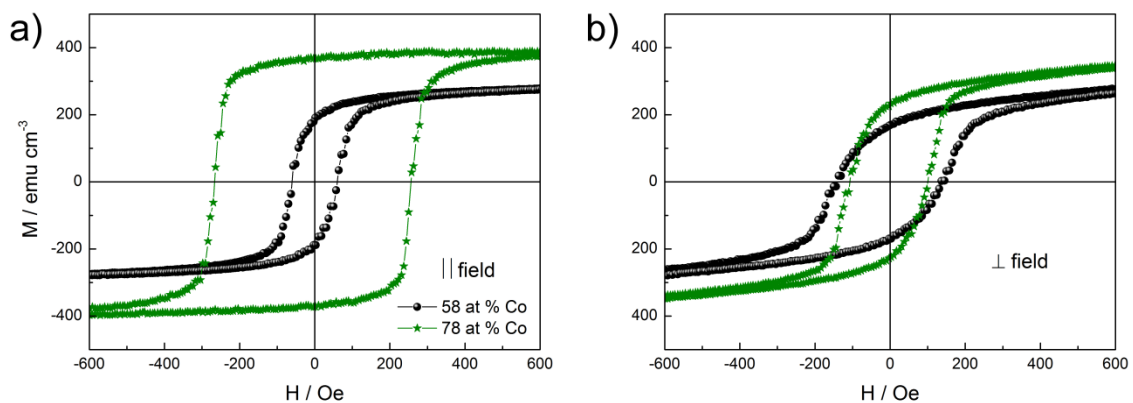


Figure 6. Room-temperature hysteresis loops measured by VSM applying the magnetic field along (a) the in-plane direction and (b) the perpendicular-to-plane direction.

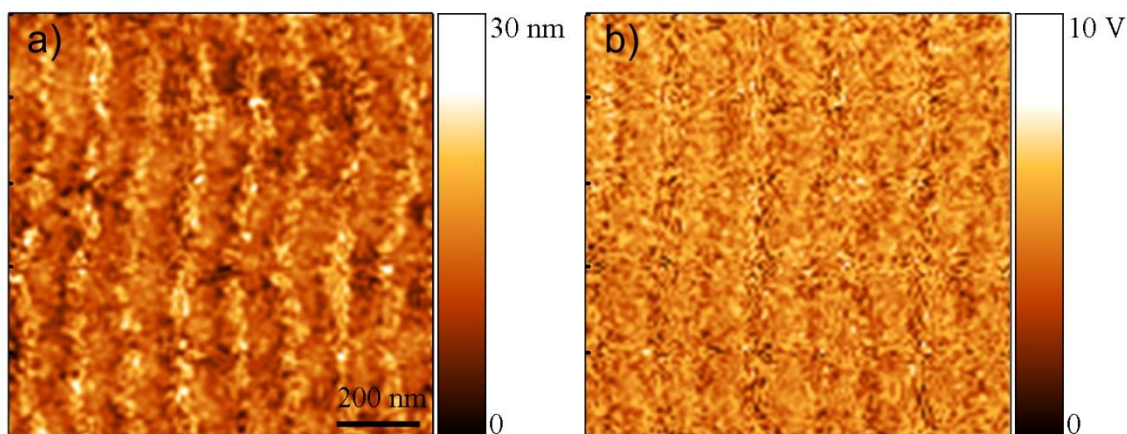


Figure 7. a) AFM and b) MFM images taken at the cross-section of Co-In films obtained at $j = -12 \text{ mA cm}^{-2}$ (58 at% Co).

4. Conclusions

Co-In nanolayered films were obtained by direct current electrodeposition on Au surfaces. TEM investigations of the films' cross-section showed the occurrence of self-assembled nanolayers along the entire deposit thickness. The layers were not compositionally homogeneous but Co- and In-rich regions coexisted in it. Moreover, each layer showed a columnar structure. A stripe-like magnetic patterning developed as a consequence of the nanolaminated structure. The possibility to electrodeposit, under direct current conditions, a system that spontaneously features a spatio-temporal pattern with micrometer lateral sizes over its surface coupled to a magnetically-patterned nanolayered vertical structure, represents a breakthrough in the field of nanocomposites science.

Acknowledgements

This work has been partially funded by the 2014-SGR-1015 project from the Generalitat de Catalunya and the MAT2014-57960-C3-1-R (co-financed by the Fondo Europeo de

Desarrollo Regional, FEDER) from the Spanish Ministerio de Economía y Competitividad (MINECO). Dr. Eva Pellicer is grateful to MINECO for the “Ramon y Cajal” contract (RYC-2012-10839).

References

- [1] B.M. Clemens, H. Kung, S.A. Barnett, Structure and strength of multilayers, *MRS Bull.* 24 (1999) 20–26.
- [2] J.J. Zhang, M.X. Wang, J. Yang, Q.X. Liu, D.J. Li, Enhancing mechanical and tribological performance of multilayered CrN/ZrN coatings, *Surf. Coat. Technol.* 201 (2007) 5186–5189.
- [3] G.S. Hickey, S.-S. Lih, T.W. Barbee Jr., Development of nanolaminate thin-shell mirrors, *Proc. SPIE* 4849 (2002) 63–76.
- [4] J. Kim, J.-K. Kim, M. Kim, F. Herrault, M.G. Allen, Microfabrication of toroidal inductors integrated with nanolaminated ferromagnetic metallic cores, *J. Micromech. Microeng.* 23 (2013) 114006.
- [5] W. Li, B. Kabius, O. Auciello, Science and technology of biocompatible thin films for implantable biomedical devices, *Proceedings of the IEEE 2010 Annual International Conference of the Engineering in Medicine and Biology Society (EMBC)*, 2010, pp. 6237–6242.
- [6] Y.Y. Tse, D. Babonneau, A. Michel, G. Abadias, Nanometer-scale multilayer coatings combining a soft metallic phase and a hard nitride phase: study of the interface structure and morphology, *Surf. Coat. Technol.* 180–181 (2004) 470–477.

- [7] K. Ikeda, K. Kobayashi, M. Fujimoto, Multilayer nanogranular magnetic thin films for GHz applications, *J. Appl. Phys.* 92 (2002) 5395–5400.
- [8] J.W. Elam, Z.A. Sechrist, S.M. George, ZnO/Al₂O₃ nanolaminates fabricated by atomic layer deposition: growth and surface roughness measurements, *Thin Solid Films* 616 (2002) 43–55.
- [9] I. Iatsunskiy, E. Coy, R. Viter, G. Nowaczyk, M. Jancelewicz, I. Baleviciute, K. Załęski, S. Jurga, Study on structural, mechanical, and optical properties of Al₂O₃–TiO₂ nanolaminates prepared by atomic layer deposition, *J. Phys. Chem. C* 119 (2015) 20591–20599.
- [10] G. Balakrishnan, P. Kuppusami, D. Sastikumar, Growth of nanolaminate structure of tetragonal zirconia by pulsed laser deposition. *J. II Song, Nano. Res. Lett.* 8 (2013) 82.
- [11] A. Misra, R.G. Hoagland, Plastic flow stability of metallic nanolaminate composites, *J. Mater. Sci.* 42 (2007) 1765–1771.
- [12] K.V. Manukyan, B.A. Mason, L.J. Groven, Y.-C. Lin, M. Cherukara, S.F. Son, A. Strachan, A.S. Mukasyan, Tailored reactivity of Ni+Al nanocomposites: microstructural correlations, *J. Phys. Chem. C* 116 (2012) 21027–21038.
- [13] F. Ebrahimi, A.J. Liscano, Microstructure/mechanical properties relationship in electrodeposited Ni/Cu nanolaminates, *Mater. Sci. Eng. A301* (2001) 23–34.
- [14] L. Péter, L. G.L. Katona, Z. Berényi, K. Vad, G.A. Langer, E. Toth-Kadar, J. Padar, L. Pogany, I. Bakonyi, Electrodeposition of Ni–Co–Cu/Cu multilayers: 2. Calculations of the element distribution and experimental depth profile analysis. *Electrochim. Acta* 53 (2007) 837–845.

- [15] H. Zhang, L. Liu, J. Bai, X. Liu, Corrosion behavior and microstructure of electrodeposited nano-layered Ni–Cr coatings, *Thin Solid Films* 595 (2015) 36–40.
- [16] L. B. Freund, S. Suresh, *Thin Film Materials: Stress, Defect Formation and Surface Evolution*, Cambridge University Press, 2004.
- [17] D.C. Meyer, A. Klingner, T. Holz, P. Paufler, Self-organized structuring of W/C multilayers on Si substrate, *Appl. Phys. A: Mater. Sci. Process.* 69 (1999) 657–659.
- [18] *Modern electroplating*, Ed. M. Schlesinger, M. Paunovic, 5th ed. John Wiley & Sons Inc.: New Jersey, 2010.
- [19] D. Rafaja, C. Schimpf, T. Schucknecht, V. Klemm, L. Péter, I. Bakonyi, Microstructure formation in electrodeposited Co–Cu/Cu multilayers with GMR effect: Influence of current density during magnetic layer deposition, *Acta Mater.* 59 (2011) 2992–3001.
- [20] J. Zhang, S. Agramunt-Puig, N. Del-Valle, C. Navau, M.D. Baró, S. Estradé, F. Peiró, S. Pané, B.J. Nelson, A. Sánchez, J. Nogués, E. Pellicer, J. Sort, Tailoring staircase-like hysteresis loops in electrodeposited tri-segmented magnetic nanowires: a strategy towards minimization of interwire interactions, *ACS Appl. Mater. Interfaces* 8 (2016) 4109–4117.
- [21] B. Bozzini, D. Lacitignola, I. Sgura, Spatio-temporal organization in alloy electrodeposition: a morphochemical mathematical model and its experimental validation, *J. Sol. State Electrochem.* 17 (2013) 467–479.
- [22] I. Krastev, T. Valkova, A. Zielonka, Structure and properties of electrodeposited silver–bismuth alloys, *J. Appl. Electrochem.* 34 (2004) 79–85.

- [23] Ts. Dobrovolska, L. Veleva, I. Krastev, A. Zielonka, Composition and structure of silver-indium alloy coatings electrodeposited from cyanide electrolytes. *J. Electrochem. Soc.* 152 (2005) C137–C142.
- [24] Y. Nagamine, O. Haruta, M. Hara, Surface morphology of spatiotemporal stripe patterns formed by Ag/Sb co-electrodeposition, *Surf. Sci.* 575 (2005) 17–28.
- [25] M.A. Estrella Gutiérrez, Ts. Dobrovolska, D.A. López Sauri, L. Veleva, I. Krastev, Self-organization phenomena during electrodeposition of Co-In alloys, *ECS Trans.* 36 (2011) 275–281.
- [26] Ts. Dobrovolska, D.A. López-Sauri, L. Veleva, I. Krastev, Oscillations and spatio-temporal structures during electrodeposition of AgCd alloys, *Electrochim. Acta* 79 (2012) 162–169.
- [27] I. Krastev, Ts. Dobrovolska, U. Lačnjevac, S. Nineva, Pattern formation during electrodeposition of indium–cobalt alloys, *J. Sol. State Electrochem.* 16 (2012) 3449–3456.
- [28] I. Golvano-Escobal, B. Özkale, S. Suriñach, M.D. Baró, T. Dobrovolska, I. Krastev, S. Pané, J. Sort, E. Pellicer, Self-organized spatio-temporal micropatterning in ferromagnetic Co–In films, *J. Mater. Chem. C* 2 (2014) 8259–8269.
- [29] P.L. Cavallotti, B. Bozzini, L. Nobili, G. Zangari, Alloy electrodeposition for electronic applications, *Electrochim. Acta* 39 (1994) 1123–1131.
- [30] Y. Wang, Y. Cao, M. Wang, S. Zhong, M.-Z. Zhang, Y. Feng, R.-W. Peng, X.-P. Hao, N.-B. Ming, Spontaneous formation of periodic nanostructured film by electrodeposition: Experimental observations and modeling, *Phys. Rev. E* 69 (2004) 021607.

- [31] S.-I. Baik, A. Duhin, P.J. Phillips, R.F. Klie, E. Gileadi, D.N. Seidman, N. Eliaz, Atomic-scale structural and chemical study of columnar and multilayer Re–Ni electrodeposited thermal barrier coating, *Adv. Eng. Mater.* 18 (2016) 1133–1144.
- [32] I. Krastev, T. Dobrovolska, Pattern formation during electrodeposition of alloys, *J. Solid State Electrochem.* 17 (2013) 481–488.
- [33] L. Peraldo Bicelli, B. Bozzini, C. Mele, L. D'Urzo, A review of nanostructured aspects of metal electrodeposition, *Int. J. Electrochem. Sci.* 3 (2008) 356–408.